

# Synthesis, characterization and catalytic properties of vanadium substituted hexagonal mesoporous aluminophosphate molecular sieves

Susanta K. Mohapatra and Parasuraman Selvam\*

Department of Chemistry, Indian Institute of Technology, Bombay, Powai, Mumbai 400076, India

Received 24 September 2003; accepted 5 December 2003

Vanadium substituted hexagonal mesoporous aluminophosphate (VHMA) molecular sieves were synthesized hydrothermally. Various physicochemical studies, *viz.*, XRD, TEM, DRUV–VIS, EPR, N<sub>2</sub> sorption were used to find the location of vanadium ions in the VHMA matrix and to check the mesoporosity of the sample. The catalytic activity of VHMA was evaluated, under mild reaction conditions, for the oxidation of cyclohexane reaction, which mainly gave cyclohexanol and cyclohexanone along with a very small amount of a secondary product, *viz.*, cyclohexyl acetate. A comparative study, with other vanadium containing molecular sieves, *viz.*, VMCM-41, VAPO-5 and VS-1, on the application of VHMA catalyst reveal that the latter exhibits excellent activity, selectivity and stability to leaching for the oxidation reaction of cycloalkanes, including bulkier molecules such as cyclododecane.

**KEY WORDS:** mesoporous; aluminophosphates; vanadium; cycloalkanes; cyclohexane; cyclododecane.

## 1. Introduction

Vanadium-based materials are known to be highly efficient catalysts in many homogeneous oxidation reactions [1,2]. However, these soluble catalysts often pose a serious threat on the practical utility while the use of heterogeneous catalysts offer several advantages with respect to easy recovery and recycling of catalysts as well as minimization of undesired toxic wastes. In view of major environmental and ecological concerns, in recent years, scientific community attempted to develop cleaner, environmentally benign routes by way of replacing traditional stoichiometric organic synthesis or conventional homogeneous route by heterogeneous catalysis-based processes. In order to overcome the specific problems of vanadium-based stoichiometric or homogeneously catalyzed process, several vanadium-based heterogeneous catalysts such immobilized metal complexes within a zeolite matrix or by supporting the active species with various supports, *viz.*, polymers, SiO<sub>2</sub> etc., have been reported [3–6]. However, in many cases leaching of active metal species was noticed, and hence, isomorphous substitution of active metal ions, e.g., V<sup>4+</sup> and/or V<sup>5+</sup>, in the framework structure of microporous molecular sieves has been employed [7–13]. However, the small pore opening of these microporous catalysts restricts their applications for processes dealing with bulky molecules. On the other hand, the discovery of a new family (M41S) of mesoporous molecular sieves, synthesized using liquid crystal templates, has opened up new opportunities in catalysis [14]. It consists of three members, *viz.*, hexagonal MCM-41 with unidimensional

pores, cubic MCM-48 with three dimensional pore apertures and thermally unstable lamellar MCM-50. These mesoporous-based materials have several advantages such as wide range of pore sizes (20–200 Å) and very high surface area (700–1500 m<sup>2</sup> g<sup>-1</sup>) [15]. Various transition metal substituted mesoporous molecular sieves have been reported, and are also widely used in many catalytic applications [15–22]. Several vanadium-based molecular sieves with MCM-41 and MCM-48 structures [19–22] as well as HMS, SBA-1 and SBA-15 structures [23–25] have successfully been synthesized. Although, all these materials exhibit high catalytic activity for many organic transformations dealing with bulky organic substrates [26–29], they still suffer from the problem of leaching active metal ions under the reactions conditions. In order to overcome these typical problems in mesoporous silicate molecular sieves, the current interest is to prepare their aluminophosphate analogues. Luan *et al.* [30] have reported the synthesis and characterization of vanadium substituted hexagonal mesoporous aluminophosphate (VHMA) molecular sieves. However, till now the catalytic properties of VHMA have not been evaluated. Hence, in this letter, we present a detailed study on the synthesis and characterization and catalytic properties of VHMA molecular sieves. Furthermore, the prepared materials have higher thermal stability (823 K) than that reported (673 K) by Luan *et al.* [30].

## 2. Experimental

### 2.1. Starting materials

Phosphoric acid (85%, Qualigens); aluminum isopropoxide (97%, Merck); tetramethyl ammonium

\* To whom correspondence should be addressed.  
E-mail: selvam@iitb.ac.in

hydroxide (TMAOH, 25 wt% in water, Aldrich); cetyltrimethylammonium chloride (CTAC, 25 wt% in water, Aldrich); fumed silica (99.8%, Aldrich); cetyltrimethylammonium bromide (CTAB, 99%, Aldrich); sodium hydroxide (NaOH, 98%, Loba); vanadyl sulfate (99%, Aldrich); triethylamine (99.5%, Thomas Baker); pseudoboehmite (70%, Vista); Tetrapropylammonium bromide (TPAB, 98%, Lancaster); cyclohexane (99.5%, Merck); methyl ethyl ketone (MEK, 99.5%, SD fine); glacial acetic acid (>99%, Fischer); cyclododecane (99%, Lancaster).

## 2.2. Synthesis

The synthesis of VHMA was carried out hydrothermally as per the following procedure. First, phosphoric acid was diluted with water; to this aluminum isopropoxide was added under constant stirring followed by the addition of aqueous solution of vanadyl sulfate. The resulting mixture was stirred at 343 K for 1 h and then TMAOH was added dropwise. After few hours of stirring, CTAC was added dropwise and the stirring was continued for another 12 h. The pH of the gel was maintained at 10. The final gel having a molar composition of:  $\text{Al}_2\text{O}_3:\text{P}_2\text{O}_5:x\text{V}_2\text{O}_5:\text{CTAC}:2.8\text{TMAOH}:70\text{H}_2\text{O}$  was kept in a Teflon-lined autoclave and heated in an air oven at 373 K for 72 h for crystallization. By varying the value of “x” from “0.01 to 0.08”, various ([Al + P]/V) molar ratio samples, viz., VHMA(200), VHMA(100), VHMA(50) and VHMA(25) were prepared. The resultant solid product was washed repeatedly with distilled water, filtered and dried at 343 K for 12 h. The calcination was performed at 823 K for 1 h in a flow of  $\text{N}_2$ , followed by 2 h in  $\text{O}_2$ . For a comparison, mesoporous VMCM-41 [31] and microporous, VS-1 [32] and VAPO-5 [33] catalysts were also synthesized hydrothermally as per the reported procedures with the following typical gel composition: VMCM-41 –  $\text{SiO}_2:0.135(\text{CTA})_2\text{O}:0.075(\text{TMA})_2\text{O}:0.13\text{Na}_2\text{O}:68\text{H}_2\text{O}:0.01\text{V}_2\text{O}_5$  (Si/V = 50); VS-1 –  $\text{SiO}_2:0.5\text{Na}_2\text{O}:0.5(\text{TPA})_2\text{O}:100\text{H}_2\text{O}:0.01\text{V}_2\text{O}_5$  (Si/V = 50); and VAPO-5 –  $0.098\text{Al}_2\text{O}_3:0.1\text{P}_2\text{O}_5:0.075\text{Pr}_3\text{N}:4\text{H}_2\text{O}:0.039\text{V}_2\text{O}_5$  ([Al + P]/V = 50). The XRD patterns of VAPO-5 and VS-1 showed well crystallized AFI and MFI topology, respectively [34,35].

## 2.3. Characterization

The as-synthesized and calcined samples were characterized using several analytical and spectroscopic techniques. Powder X-ray diffraction (XRD) patterns were recorded on a Rigaku-miniflex diffractometer using a nickel filtered  $\text{CuK}\alpha$  radiation ( $\lambda = 1.5418 \text{ \AA}$ ) and a step size of  $0.02^\circ$ . Transmission electron micrograph (TEM) image was recorded on a Philips 200 microscope operated at 160 kV. The sample (in fine powdered form) was dispersed in ethanol with sonication (Oscar ultrasonics) and placed a drop of it on a carbon coated

copper grid (300 mesh; Sigma-Aldrich). The elemental analysis of the various samples was carried out by inductively coupled plasma-atomic emission spectroscopy ICP-AES technique on Labtam Plasma Lab 8440 equipment. Thermogravimetry/differential thermal analysis (TG–DTA) measurements were performed using ~15 mg of the sample on a Dupont 9900/2100 system under nitrogen atmosphere ( $40 \text{ mL min}^{-1}$ ) with a heating rate of  $10 \text{ K min}^{-1}$ . Surface area analysis was performed on a Sorptomatic-1990 instrument. Before measurement, the calcined sample was evacuated at 523 K for 12 h under vacuum ( $10^{-3}$  Torr). The surface area was calculated using the Brunauer–Emmett–Teller (BET) method and the pore size was calculated using the Horvath–Kawazoe method. The pore volume was determined from the amount of  $\text{N}_2$  adsorbed at  $P/P_0 = 0.5$ . Diffuse reflectance ultraviolet and visible (DRUV–VIS) spectra were recorded on UV-260 Shimadzu spectrophotometer with Whatman-40 filter paper as standard. Electron spin resonance (ESR; Varian E-112) spectra were recorded both at room temperature (300 K) and liquid  $\text{N}_2$  temperature (77 K).

## 2.4. Oxidation of cyclohexane

### 2.4.1. Reaction procedure

The oxidation of cyclohexane (18 mmol) was carried out in presence of 5 mmol initiator (MEK) at 373 K for 12 h under atmospheric pressure using 50 mg of the catalyst with 18 mmol of oxidant (30%  $\text{H}_2\text{O}_2$ ) and 10 mL of solvent (acetic acid). Oxidation of cyclododecane (12 mmol) was carried out under similar conditions as mentioned above for cyclohexane reaction but the only change made is for cyclododecane mixed solvents (5 mL acetic acid + 5 mL  $\text{CH}_2\text{Cl}_2$ ) were utilized to make a homogeneous reaction mixture. After the reaction, the catalyst was separated and the products were extracted with ether and analyzed by gas chromatography (GC; Nucon) with Carbowax column. Further confirmation of oxidation products were confirmed by GC-MS (Hewlett Packard G1800A) equipped with a HP-5 capillary column.

### 2.4.2. Recycling studies

After the first run, the catalyst was filtered, washed with distilled water three times, dried in an air-oven, and then activated at 773 K for 6 h, and used for the subsequent recycling studies.

### 2.4.3. Washing studies

The calcined catalyst (100 mg) was washed with 25 mL 1 M ammonium acetate for 12 h at room temperature under constant stirring. Then, the catalyst was filtered, washed, dried and activated at 773 K for 6 h. This catalyst is noted as washed catalyst.

#### 2.4.4. Filtrate and quenching studies

In the filtrate study, the reaction was carried out with the filtrate collected at room temperature, i.e., the reaction mixture was cooled to RT and then filtered. On the other hand the quenching studies, the reaction was carried out with the filtrate collected in the hot condition.

### 3. Results and discussion

All the as-synthesized and calcined VHMA samples were white in color. The as-synthesized VMCM-41 sample was also white in color and so was the fresh calcined VMCM-41 sample, but the calcined sample gradually changed to faint yellowish-orange on exposure to atmosphere at room temperature. Table 1 summarizes ICP-AES data of calcined HMA and VHMA samples. The increase in molar ratios in calcined samples compared to the starting gel indicates that some of the vanadium species are lost in mother liquor during the synthesis. The decrease in Al/P molar ratios with increase in vanadium content in the sample suggests the incorporation of vanadium in aluminum sites. XRD patterns of as-synthesized HMA as well as VHMA samples (figure 1) showed well-resolved reflections corresponding to mesoporous hexagonal system [36–38]. The increase in unit cell parameter of VHMA samples (table 1) as compared to HMA indicates a possible substitution of  $V^{4+}/V^{5+}$  in the aluminophosphate network owing to larger crystal radii of the  $V^{4+}$  (0.59 Å) or  $V^{5+}$  (0.495 Å) than  $Al^{3+}$  (0.52 Å) and  $P^{5+}$  (0.32 Å) [39]. Figure 2 showed the diffraction pattern of the corresponding calcined samples. It can be deduced from this figure that upon calcination a decrease in unit cell dimension values was observed for all the samples due to the contraction of the framework after the removal of the surfactants. In addition to this, higher order peaks, viz., 110, 200 and 210 disappeared and only a broad single reflection corresponding to 100 peak was observed. Similar observations were reported by most of the researchers on HMA and concluded that this may be due to finite size effects of very fine particle morphology or due to the disordered hexagonal structure [40].

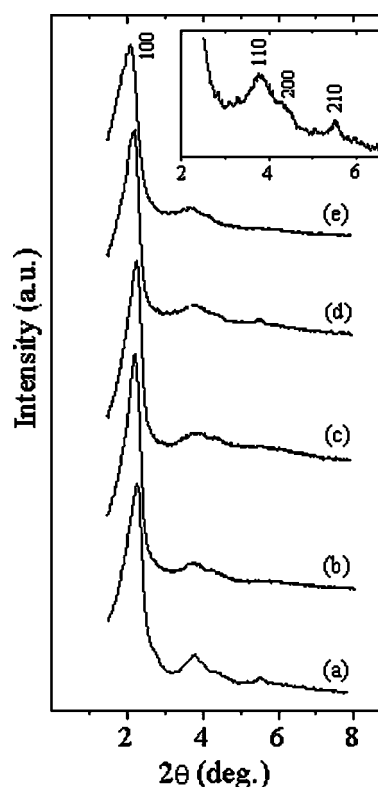


Figure 1. XRD patterns of as-synthesized: (a) HMA, (b) VHMA(200), (c) VHMA(100), (d) VHMA(50) and (e) VHMA(25).

However, TEM image (figure 3) of calcined VHMA(50) showed disordered hexagonal array of arrangements. A representative  $N_2$  sorption isotherm of calcined VHMA(50) was shown in figure 4. It follows type IV isotherm typical of mesoporous materials [41]. As the relative pressure increases ( $P/P_0 > 0.2$ ), the isotherm exhibits an inflection characteristic of capillary condensation within the mesopores. Adsorption at low relative pressures ( $P/P_0 < 0.2$ ) is caused by monolayer adsorption of  $N_2$  on the walls of the mesopores. At  $P/P_0 = 0.5$  the pore volume was calculated as  $0.42 \text{ cm}^3 \text{ g}^{-1}$  with specific surface area,  $870 \text{ m}^2 \text{ g}^{-1}$ . A narrow pore size distribution was observed (figure 4, inset) with mesopore diameter 26 Å. These values are significantly less than vanadium-free HMA samples ( $S_{\text{BET}} = 985 \text{ m}^2 \text{ g}^{-1}$ ; pore

Table 1  
XRD and ICP-AES data of VHMA with different vanadium content

Samples	[Al+P]/V <sup>a</sup>		V (wt%)	Al/P <sup>a</sup>	$a_0$ (Å) <sup>b</sup>	
	Synthesis gel	Calcined			As-synthesized	Calcined
HMA	–	–	–	1.34	45.4	33.7
VHMA(200)	200	390	0.30	1.33	46.2	33.1
VHMA(100)	100	212	0.55	1.33	46.5	35.6
VHMA(50)	50	131	0.90	1.32	47.2	35.7
VHMA(25)	25	79	1.75	1.31	47.8	36.9

<sup>a</sup>Molar ratio.

<sup>b</sup>Average unit cell parameter.

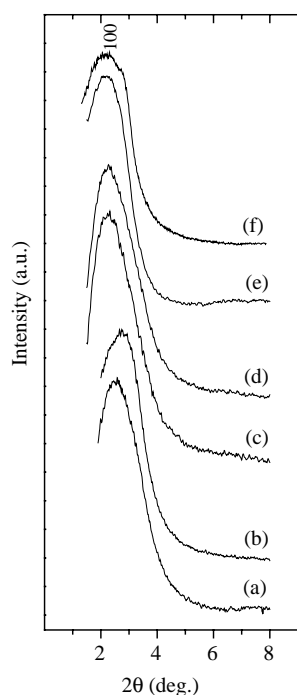


Figure 2. XRD patterns of calcined: (a) HMA, (b) VHMA(200), (c) VHMA(100), (d) VHMA(50), (e) VHMA(25) and (f) calcined VHMA(50) after cyclohexane oxidation.

volume =  $0.47 \text{ cm}^3 \text{ g}^{-1}$ ; pore size =  $25 \text{ \AA}$ ) indicating the pore blockage by the formation of extra-framework species. The calcined VMCM-41 is also showed mesoporous in nature. Further,  $\text{N}_2$  adsorption–desorption (sorption) analysis confirmed the mesoporous nature of all the samples (table 2).

FT-IR spectra (not reproduced here) of as-synthesized VHMA samples showed characteristic bands corresponding to mesoporous aluminophosphate matrix along with template molecules [42]. On the other hand, FT-IR spectra (not reproduced here) calcined samples indicate the absence of bands at  $2827$ ,  $2861$  and  $1480 \text{ cm}^{-1}$  suggesting complete removal of the template molecules from the matrix. TG analysis of all the as-synthesized VHMA samples showed a total weight loss of  $55$ – $60\%$  in three different stages (not reproduced here), which is typical of mesoporous materials, corresponding to adsorbed water, occluded surfactant and

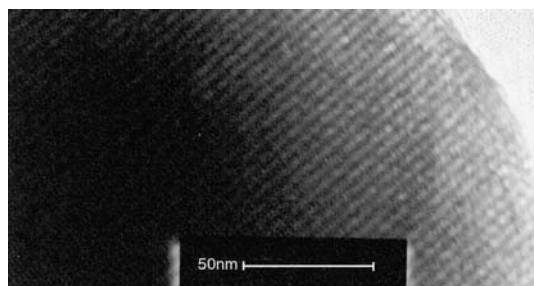


Figure 3. TEM image of calcined VHMA(50).

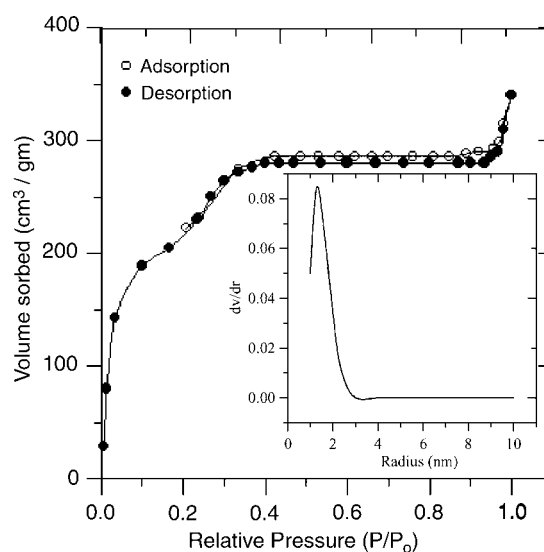


Figure 4. Representative nitrogen sorption isotherms of calcined VHMA(50). The inset indicate the pore size distribution.

charge compensating organic base [43]. These processes were well supported by corresponding endothermic and exothermic transitions in DTA trace (not reproduced here). Likewise, calcined VHMA samples showed a weight loss of  $20$ – $25\%$  in a single step (TG is not reproduced here), which is accompanied by an endothermic transition (DTA is not reproduced here) around  $433 \text{ K}$  corresponding to adsorbed water molecules.

DRUV–VIS spectra of as-synthesized VHMA samples (not reproduced here) with different vanadium contents have broad bands in the range  $200$ – $500 \text{ nm}$  with a maximum at  $280$ – $290 \text{ nm}$  regions. The broadness of the spectra is also increases with increase in vanadium content, e.g., VHMA(25), which is typical for charge transfer transitions of  $\text{V}^{5+}$  ions in a tetrahedral coordination surrounded by  $\text{O}^{2-}$  ions [19,22]. In addition to these features, they also show very weak absorption bands in  $600$ – $700 \text{ nm}$  regions, which may be attributed to d–d transitions of vanadyl  $\text{V}^{4+}$  ions [19]. Although, most of the  $\text{V}^{4+}$  ions in the vanadium source used for the synthesis are oxidized to  $\text{V}^{5+}$  ions during synthesis procedure, such species may, however, be noticed when concentration of the tetravalent vanadium is high such

Table 2  
Nitrogen sorption data of calcined VHMA and VMCM-41

Catalysts	$S_{\text{BET}}$ ( $\text{m}^2 \text{ g}^{-1}$ )	Pore volume ( $\text{mL g}^{-1}$ )	H–K pore diameter ( $\text{\AA}$ )
HMA	985	0.47	25
VHMA(200)	960	0.50	25
VHMA(100)	945	0.46	26
VHMA(50)	930	0.42	26
VHMA(50) <sup>a</sup>	910	0.42	26
VHMA(25)	910	0.43	27

<sup>a</sup>Spent (or used) catalyst.

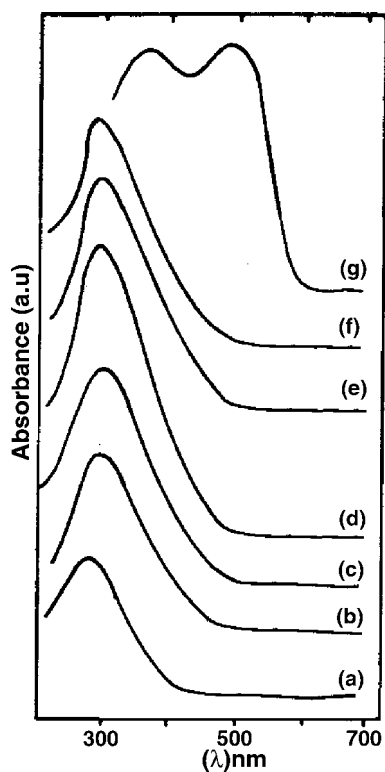


Figure 5. DRUV-VIS spectra of calcined: (a) VHMA(200), (b) VHMA(100), (c) VHMA(50), (d) VHMA(25), (e) washed VHMA(50), (f) calcined VHMA(50) after cyclohexane oxidation and (g)  $V_2O_5$ .

as in the case of VHMA(25), which is clearly evidenced from ESR data presented below. Figure 5 depicts DRUV-VIS spectra of calcined VHMA, and that no significant change was observed even after calcinations or after washing and recycling experiments. This observation indicates that the stability of the vanadium species in the tetrahedral framework structure. ESR spectra of as-synthesized VHMA, both at 300 and 77 K (not reproduced here), showed identical patterns with variable intensities suggesting the presence of  $V^{4+}$  species in

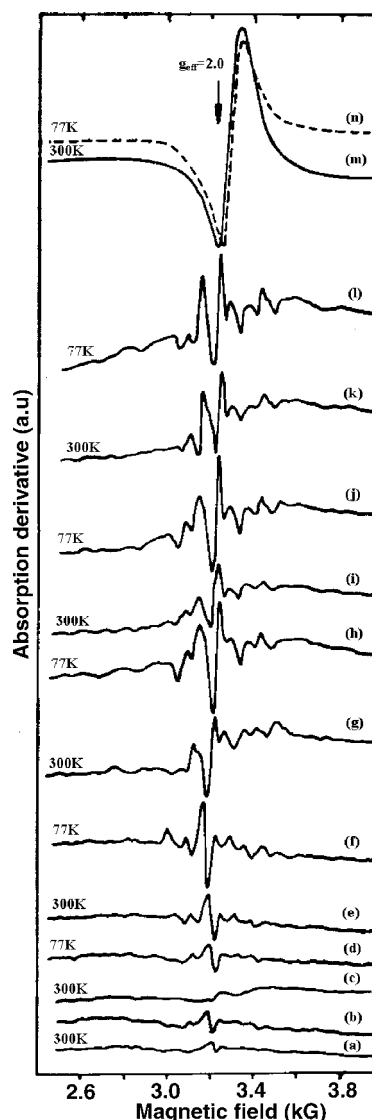


Figure 6. ESR spectra of calcined: (a,b) VHMA(200), (c,d) VHMA(100), (e,f) VHMA(50), (g,h) VHMA(25), (i,j) washed VHMA(50), (k,l) calcined VHMA(50) after cyclohexane oxidation and (m,n) bulk  $V_2O_5$ .

Table 3  
Oxidation of cyclohexane over VHMA

Catalysts	Conversion (wt%)	Selectivity (wt%)		
		-ol	-one	Others <sup>a</sup>
VHMA(200)	48.8	93.4	1.5	5.1
VHMA(100)	68.0	93.0	2.0	5.0
VHMA (50)				
Calcined	95.0	91.7	2.7	5.6
Filtrate	13.7	86.5	1.0	12.5
Quenched solution	12.0	83.2	4.5	12.3
Recycled <sup>b</sup>	88.3	87.0	10.8	2.2
Washed	90.0	83.1	13.8	3.1
VHMA(25)	98.7	88.8	4.0	7.2
HMA	9.8	82.8	1.3	15.9
Blank	9.0	78.1	—	21.9

<sup>a</sup>Mainly contains cyclohexyl acetate.

<sup>b</sup>3rd cycle (or 4th run).

all these samples, as  $V^{5+}$  is ESR inactive [20]. However, as expected, the signal intensity increases ( $\sim 2$  times) with decreasing temperature, i.e., on going from 300 to 77 K, indicating the paramagnetic nature of  $V^{4+}$  ions. The spectra showed well-resolved hyperfine structure caused by the vanadium nucleus ( $I = 7/2$ ) with calculated parameters, viz.,  $g_{\parallel} = 1.938$ ,  $A = 191\text{G}$ ,  $g_{\perp} = 1.99$  and  $A = 71\text{G}$ ; where  $A$  is hyperfine splitting parameters, which are in line with  $V^{4+}$  substituted molecular sieves [30]. The presence of hyperfine pattern in these samples indicates the vanadium ions are isolated in the matrix, whereas oligomeric  $V_2O_5$  like species gives rise to a singlet [7]. The corresponding calcined samples also showed similar ESR pattern (figure 6) indicating incomplete oxidation of  $V^{4+}-V^{5+}$  even after calcinations process.

Table 3 summarizes the results of cyclohexane oxidation over various VHMA. It can be seen from this table that with increasing vanadium content, the conversion increases. All the catalysts gave mainly two (primary) products, viz., cyclohexanol and cyclohexanone, with small amounts of secondary products such as cyclohexyl acetate. It is, however, to be noted here that vanadium-free HMA as well as without catalyst (blank), the reaction showed only  $\sim 10\%$  conversion. Thus, the observed high activity of VHMA could be attributed to the presence of isolated tetrahedral  $V^{4+}/V^{5+}$  ions in the matrix. In order to check the reusability of the catalyst, recycling experiments were carried out over VHMA(50) catalyst (figure 7). It can be seen from this figure that there is a small loss in activity during the first recycle (or 2nd run) and thereafter the activity remains nearly the same. The loss in activity could be attributed to the leaching of loosely bound non-framework vanadium species under the reaction conditions. This observation is well supported by washing studies, where ICP-AES analysis of washed solution under reaction conditions of calcined VHMA(50) gave about 5–7% of the total vanadium present in the catalyst. However, no loss in

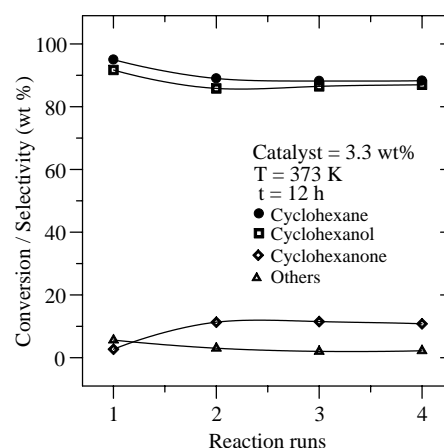


Figure 7. Recycling results of the oxidation of cyclohexane over VHMA(50).

vanadium was detected for the recycled sample, and therefore a steady activity after the first recycle is noticed suggesting that the stabilization of vanadium ions in the aluminophosphate matrix. Thus, VHMA truly behaves as heterogeneous catalyst. Furthermore, the structure of the catalyst remains intact even after the recycling experiments, as there is no significant change in the observed XRD patterns (figure 2f), and porosity is not altered much (see table 2) even after third recycle.

Table 4 presents the results of the oxidation of a bulkier cycloalkane (cyclododecane) over VHMA (table 4). It is interesting to note that the mesoporous aluminophosphate catalyst showed very good conversion and selectivity for the oxidation of cyclododecane as well. Further, the catalyst showed much higher activity as compared to many other catalysts reported for the oxidation of cyclododecane [26,44]. However, a decrease in selectivity of cyclododecanol was observed which may be due to the lower diffusion rate of the bulky cyclododecanol, which in contrast with cyclohex-

Table 4  
Oxidation of cyclododecane over various vanadium containing catalysts<sup>a</sup>

Catalysts	Conversion (wt%)	Selectivity (wt%)		
		-ol	-one	Others <sup>b</sup>
VHMA(50)				
Calcined	90.8	75.0	18.1	6.9
Recycled <sup>c</sup>	86.0	72.5	23.2	4.3
VMCM-41(50)				
Calcined	93.8	80.0	12.0	8.0
Recycled <sup>c</sup>	81.6	72.8	20.5	6.7
VAPO-5(50)	22.0	71.0	15.0	14.0
VS-1(50)	18.0	65.5	17.5	17.0

<sup>a</sup>Reaction conditions: 373 K; 12 h; substrate: oxidant ( $H_2O_2$ ) = 1:1; catalyst = 50 mg (2.48 wt%); solvent = (acetic acid 5 mL +  $CH_2Cl_2$  5 mL); MEK = 5 mmol.

<sup>b</sup>Mainly contains cyclohexyl acetate.

<sup>c</sup>3rd cycle (or 4th run).

ane oxidation. On the other hand, a similar observation was also made upon recycling studies, where VHMA showed the same activity for the oxidation of cyclododecane after first cycle. For a comparison, the oxidation of cyclododecane was also carried out over mesoporous VMCM-41 as well as microporous VAPO-5 and VS-1. As can be seen from table 4 that the vanadium-containing aluminophosphate (VAPO-5) and silicate (VS-1) catalysts showed only meager activity owing to their pore size restriction for the bulky cyclododecane. On the other hand, calcined VMCM-41(50) showed comparable activity, however, showed a significant loss in activity upon cycling. This could be attributed to the leaching of large amounts of active vanadium species from the matrix (15–20%).

#### 4. Conclusion

In conclusion, vanadium substituted mesoporous aluminophosphate molecular sieves were successfully synthesized and characterized. Various characterization techniques suggest the presence of both isolated  $V^{4+}$  /  $V^{5+}$  ions in tetrahedral framework sites. The catalyst showed excellent activity and reusability for the oxidation of cyclohexane under mild reaction conditions. It was also demonstrated that VHMA oxidizes bulkier substrates like cyclododecane. Furthermore, the catalyst can be considered as viable alternatives to the homogeneous catalysts due to their easy recovery and recycling, thus it opening up a new possibility in the area of fine chemicals, which deals with bulky organic molecules.

#### Acknowledgment

The authors thank Mr. S.E. Dapurkar for the experimental assistance, and SAIF, IIT-Bombay, for ICP-AES, TEM and EPR measurements.

#### References

- [1] L.J. Csányi, K. Jáky and G. Galbács, *J. Mol. Catal. A* 164 (2000) 109.
- [2] B.M. Choudary, V. Neeraja and M.L. Kantam, *J. Mol. Catal. A* 175 (2001) 169.
- [3] G.L. Linden and M.F. Farana, *J. Catal.* 48 (1977) 284.
- [4] S. Bhaduri, A. Ghosh and H. Khwaja, *J. Chem. Soc., Dalton Trans.* (1981) 447.
- [5] L.C. Passoni, F.J. Luna, M. Wallau, R. Buffon and U. Schuchhardt, *J. Mol. Catal. A* 134 (1998) 229.
- [6] M. Ishida, Y. Masumoto, R. Hamada, S. Nishiyama, S. Tsuruya and M. Masai, *J. Chem. Soc., Perkin Trans. 2* (1999) 847.
- [7] G. Bellussi and M.S. Rigutto, *Stud. Surf. Sci. Catal.* 85 (1994) 177.
- [8] M. Hartmann and L. Kevan, *Chem. Rev.* 99 (1999) 635.
- [9] H. Du, M. Fang, Y. Liu, S. Qiu and W. Pang, *Zeolites*, 18 (1997) 334.
- [10] B.I. Whittington and J.R. Anderson, *J. Phys. Chem.* 97 (1993) 1032.
- [11] P.R.H.P. Rao and A.V. Ramaswamy, *Appl. Catal. A* 93 (1993) 123.
- [12] T. Selvam and A.P. Singh, *J. Chem. Soc., Chem. Commun.* (1995) 883.
- [13] M.J. Haanepen and J.H.C. van Hooff, *Appl. Catal. A* 152 (1997) 183.
- [14] C.T. Kresge, M.E. Leonowicz, W.J. Roth, J.C. Vartuli and J.S. Beck, *Nature* 359 (1992) 710.
- [15] P. Selvam, S.K. Bhatia and C. Sonwane, *Ind. Eng. Chem. Res.* 40 (2001) 3237.
- [16] A. Corma, *Chem. Rev.* 97 (1997) 2373.
- [17] J.Y. Ying, C.P. Mehnert and M.S. Wong, *Angew. Chem., Int. Ed.* 38 (1999) 56.
- [18] D. Trong On, D. Desplandier-Giscard, C. Danumah and S. Kaliaguine, *Appl. Catal. A* 222 (2001) 299.
- [19] K.J. Chao, C.N. Wu, H. Chang, L.J. Lee and S.-F. Hu, *J. Phys. Chem. B* 101 (1997) 6341.
- [20] Z. Luan, J. Xu, H. He, J. Klinowski and L. Kevan, *J. Phys. Chem.* 100 (1996) 19595.
- [21] A.B.J. Arnold, J.P.M. Niederer, T.E.W. Nießen and W.F. Hölderich, *Micropor. Mesopor. Mater.* 28 (1999) 353.
- [22] M. Mathieu, P. Van Der Voort, B.M. Weckhuysen, R.R. Rao, G. Catana, R.A. Schoonheydt and E.F. Vansant, *J. Phys. Chem. B* 105 (2001) 3393.
- [23] Z. Luan, J.Y. Bae and L. Kevan, *Chem. Mater.* 12 (2000) 3202.
- [24] L.-X. Dai, K. Tabata, E. Suzuki and T. Tatsumi, *Chem. Mater.* 13 (2001) 208.
- [25] J.S. Reddy and A. Sayari, *J. Chem. Soc., Chem. Commun.* (1995) 2231.
- [26] K.M. Reddy, I. Moudrakovski and A. Sayari, *J. Chem. Soc., Chem. Commun.* (1994) 1059.
- [27] R. Neumann and A.K. Khenkin, *Chem. Commun.* (1996) 2643.
- [28] S. Gontier and A. Tuel, *J. Catal.* 157 (1995) 124.
- [29] J.S. Reddy, P. Liu and A. Sayari, *Appl. Catal. A* 148 (1996) 7.
- [30] Z. Luan, D. Zhao and L. Kevan, *Micropor. Mesopor. Mater.* 20 (1998) 93.
- [31] A. Sakthivel, S.E. Dapurkar and P. Selvam, in: *Advances in Environmental Materials*, Vol. I (*Pollution Control Materials*), eds. T. White and D. Sun (Materials Research Society, Singapore, 2001) p. 67.
- [32] T. Sen, P.R. Rajamohanan, S. Ganapathy and S. Sivasanker, *J. Catal.* 163 (1996) 354.
- [33] K. Vidya, R.J. Mahalingam and P. Selvam, *Bull. Catal. Soc. India* 1 (2002) 142.
- [34] J.M. Bennett, J.P. Cohen, E.M. Flanigen, J.J. Pluth and J.V. Smith, *ACS Symp. Ser.* 218 (1983) 109.
- [35] G.T. Kokotailo, S.L. Lawton, D.H. Olson and W.H. Meier, *Nature* 272 (1978) 437.
- [36] T. Kimura, Y. Sugahara and K. Kuroda, *Chem. Lett.* (1997) 983.
- [37] S.K. Mohapatra, F. Hussain and P. Selvam, *Catal. Lett.* 85 (2003) 217.
- [38] S.K. Mohapatra, F. Hussain and P. Selvam, *Catal. Commun.* 4 (2003) 57.
- [39] R.D. Shannon, *Acta Crystallogr. A* 32 (1976) 751.
- [40] P.T. Tanev and T.J. Pinnavaia, *Science* 267 (1995) 865.
- [41] S.J. Gregg and K.S.W. Sing, *Adsorption, Surface Area and Porosity*, 2nd ed. (Academic Press, London, 1982).
- [42] T. Kimura, Y. Sugahara and K. Kuroda, *Chem. Mater.* 11 (1999) 508.
- [43] S.K. Mohapatra and P. Selvam, *Top. Catal.* 22 (2003) 17.
- [44] D.H.R. Barton, E. Csuhai and N. Ozbalik, *Tetrahedron* 46 (1990) 3743.